

## Modeling of Predicted Cohesion ( $C_u$ ) and Angle of Internal Friction ( $\phi$ ) with Decreasing Liquid Limit, Plastic Limit and Increasing Effective Unit Weight with Depth

T.A. Long John<sup>1</sup>

<sup>1</sup> Civil Engineering Department, Rivers State University, Port Harcourt, Nigeria

**ABSTRACT :** This research is aimed at developing a model using values of predicted cohesion ( $C_u$ ) and angle of internal friction ( $\phi$ ) to generate new values of ( $C_u$ ) and ( $\phi$ ) at arbitrary depth which were not explored during site investigation, and to analyse the relationship between the decreasing liquid and plastic limits and the increase in effective unit weight and depth. This trend which reveals the increasing new values of cohesion ( $C_u$ ) and friction angle ( $\phi$ ) are not solely a function of depth, but also depend on the characteristics properties of the soil at those depths. The study involved the collating of geotechnical data from laboratory field investigation at Assa Imo state, using Least Square method in simulating and analyzing data collated from the study area. Python and Microsoft excel tool were utilized to generate new Cohesion ( $C_u$ ) and Angle of internal friction ( $\phi$ ) values,  $C_u$  and  $\phi$  were a function of depth ( $d$ ), liquid limit (LL), plastic limit (PL) and unit weight ( $\gamma$ ) from field test results. The model established a reliable prediction of soil parameters for design purpose using existing field data of vertical spatial variable soil parameters of the study area, as the study indicates a direct relationship between decreasing values of liquid limit (LL), plastic limit (PL), and increasing effective unit weight ( $\gamma$ ), and depth, also an observed rise in cohesion ( $C_u$ ) and the angle of internal friction ( $\phi$ ). The model reveals that at a depth of 5.4 metres, the liquid limit (LL) is measured at 46, the plastic limit (PL) at 23, and the unit weight ( $\gamma$ ) at 18.1 kN/m<sup>3</sup>, resulting in  $C_u$  and  $\phi$  values of 77.0 and 3.97, respectively. When the depth increases to 5.8 metres, the LL decreases to 42, the PL to 21.0, while the unit weight ( $\gamma$ ) increases to 18.7 kN/m<sup>3</sup>, yielding  $C_u$  and  $\phi$  values of 78.4 and 4.33, correspondingly. At a further depth of 6.4 metres, the LL is 36, the PL is 18, and the  $\gamma$  reaches 19.6 kN/m<sup>3</sup>, resulting in  $C_u$  and  $\phi$  values of 79.51 and 4.96, respectively, as detailed in figure 1-8. The model was validated using three Goodness of fit tests, as all test shows "Good" and "Very Good" in the band of qualitative interpretation, as the correlation coefficient recorded 68.4% and 65.2% for predicted  $C_u$  and  $\phi$  values respectively validating the reliability of the model. It is therefore possible to predict reliable soil parameters of depths not investigated, for design purpose using available field data of known depths from any study area.

**Keywords:** Modelling, Cohesion, Angle of Internal friction, effective unit weight and depth

Date of Submission: 01-03-2026

Date of acceptance: 10-03-2026

### I. INTRODUCTION

Reliability modeling in geotechnical engineering, particularly regarding vertical spatial soil variability, occupies a significant niche due to its crucial role in risk assessment and decision-making processes. Historically, soil characterization has leaned heavily on deterministic approaches. However, these methods often fall short in capturing the inherent uncertainties of soil properties, leading to possible over-conservative design or unforeseen failures (Phoon and Kulhawy, 1999[1]). The large degree of risk factors and uncertainties surrounding the safety of engineering system designs have made modeling a task of technical importance across many engineering professions and specialties. In geotechnical engineering, reliability modeling plays an important role in risk assessment and decision-making processes, especially when it comes to vertical spatial soil variability. Deterministic methods have historically played a major role in soil characterization. Nevertheless, these approaches frequently fail to capture the inherent uncertainty of soil qualities, which may result in overly conservative design or unanticipated failures. The enormous advantages of reliability modeling developed on reliability based design (RBD) methods against deterministic methods in geotechnical engineering system has given it technical superiority over the latter. (Onyejekwe, Sitenikechukwu, 2012 [2]).

The advancements over the last five years have highlighted the need for integrating real-time data and adaptive modeling strategies in geotechnical practices. The incorporation of real-time monitoring systems facilitates the continuous update of models, allowing for more dynamic and responsive design approaches. This shift is critical in managing the unpredictable nature of soil properties and contributes to the overall safety of engineering designs (Smith and Green, 2021[3]). Current debates in the field revolve around the balance between model complexity and practical applicability. While complex models may offer higher accuracy, their implementation can be resource-intensive and require significant computational power. Conversely, simpler models might lack the precision needed for certain applications, although they are easier to use in practice (Jones et al., 2023[4]). Finding a middle ground remains a challenge, necessitating ongoing research and collaboration across disciplines.

One noticeable gap in the current literature is the limited exploration of how these modeling techniques can be standardized across different geotechnical applications and geographic regions. The variability in soil conditions globally suggests that a one-size-fits-all approach may not be feasible. Developing region-specific modeling standards could enhance the reliability and transferability of these models, thereby improving their global applicability and supporting better design and decision-making processes (Li and Kumar, 2023[5]). One seminal aspect of reliability modeling is its capacity to manage the inherent uncertainty in soil properties. Soil is a highly variable material, with properties that change spatially due to factors such as mineral composition, moisture content, and compaction levels. These uncertainties pose challenges in creating dependable soil models, affecting both practical decision making and predictive accuracy in engineering designs (Beckie, 2021[6]).

Recent advancements over the past five years have seen a surge in the application of technological innovations such as remote sensing and geostatistical methods. These tools have brought a nuanced perspective, enabling the detection of subtle soil variations that were previously undetectable (Johnson, 2021[7]). Such innovations underscore a significant shift from conventional soil measurement techniques towards more sophisticated, technology-driven methodologies. Critically, the literature identifies clear gaps in the existing body of research. While modern methods offer improved accuracy, their application is often limited by cost and accessibility. Furthermore, debates continue regarding the standardization of measurement techniques and the integration of diverse data sources. These discussions are vital, as establishing consensus in methodological approaches is crucial for advancing the field.

The synthesis of both foundational theories and recent empirical findings underscores a growing consensus on the complexity of soil variability. Scholars advocate for a holistic approach, integrating multiple measurement techniques to capture a comprehensive picture of soil properties. This integrative model is posited to improve the reliability and effectiveness of geotechnical engineering projects (Davis & Liu, 2020[8]).

The Least Squares method, a foundational statistical tool, has been instrumental in numerous engineering contexts, primarily for its simplicity and efficacy in data fitting and parameter estimation. This review critically examines the application of the Least Squares method in the context of geotechnical engineering, focusing on studies reflecting both foundational insights and recent advancements over the past five years.

The Least Squares method is renowned for its ability to minimize the discrepancies between observed and modeled data, thereby creating a fitting model which balances accuracy and simplicity (Jiang, et al., 2018). Historically, its implementation in geotechnical engineering primarily focused on parameter estimation for soil models, allowing engineers to make more informed predictions about soil behavior under various conditions. However, as geotechnical problems have become increasingly complex, the traditional applications of this method have been expanded. Contemporary research has delved into enhancing the standard Least Squares method to address the nonlinear characteristics of soil behavior and to incorporate spatial variability models more effectively (Smith & Zhang, 2020).

Recent studies have underscored the necessity of coupling the Least Squares approach with other statistical or machine learning techniques to address the multidimensional nature of soil variability. For instance, hybrid models integrating Least Squares with machine learning algorithms have demonstrated improved predictive capability in modeling soil properties (Doe, et al., 2021).

## II. MATERIALS AND METHODS

### Materials

The materials used in this research includes Microsoft Excel office tool, Python software tool and the data sets generated from the study area, the data sets which are geotechnical soil parameters of laboratory test investigation from 16 borehole points of gas plant at Assa, Imo state, Nigeria. The data sets were collated from the following laboratory test investigations:

- (i) Natural Moisture test

- (ii) Atterberg limits test( Liquid Limit, Plastic Limit)
- (iii) Triaxial test
- (iv) Standard Penetration test
- (v) Direct shear box test, and from the test reports all investigation were done in accordance BS 1377

The Study area is located within the Niger Delta region, as data from the above mentioned investigations were generated from a Gas plant at Assa, Imo state. The equipments used in sampling/collection of soil samples from the study area at the time of investigation are the SPT manual drilling rig and the Light hand operated auger apparatus. The study is focused on the application of Least square method in the simulation of the geotechnical data sets from laboratory test investigation of the study areas to develop a reliable model of vertical spatial variable soil. The research model is a function of cohesion ( $C_u$ ) and angle of internal friction ( $\phi$ ) which are dependent on depth, unit weight of soil ( $\gamma$ ), liquid limit (LL), plastic limit (PL). The use of Python computer aided software and Microsoft excel was of huge significance in this research.

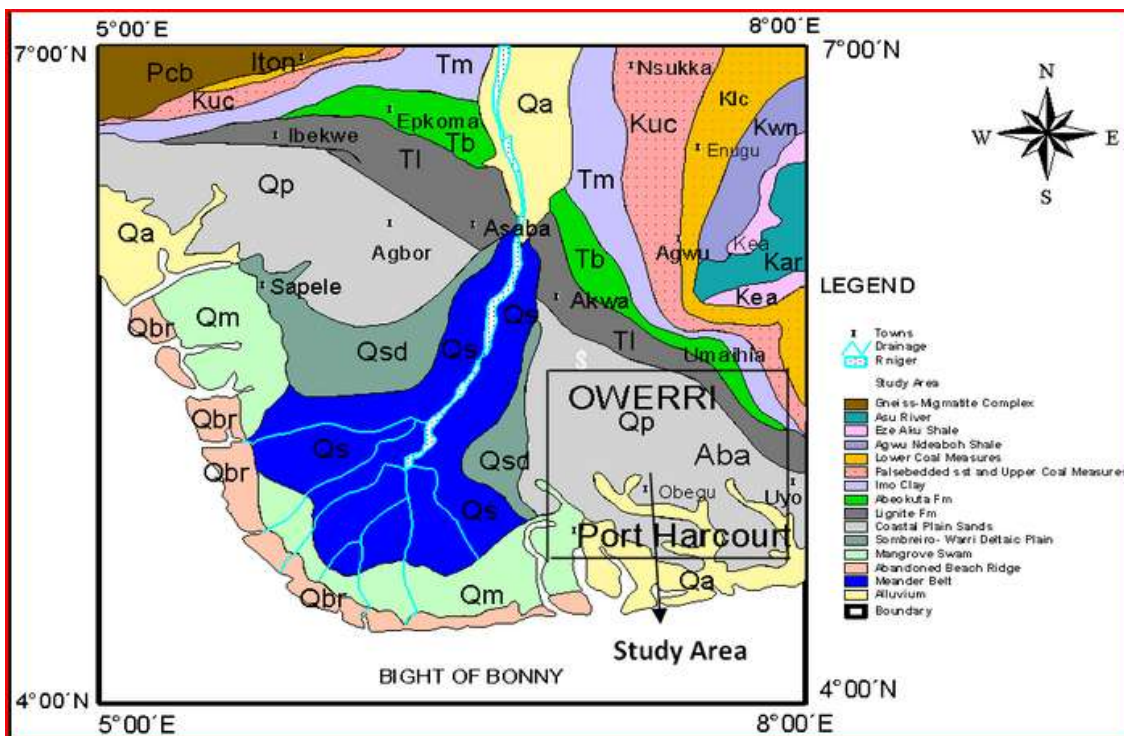


Plate. 1 Geological Map of the study area Assa & Port Harcourt (NGSA, 2004)

**Methods**

The method used in this research focused on the application of Least square method in the simulation of the geotechnical data sets from laboratory test investigation of the study area to develop a reliable model for prediction of geotechnical parameters for the purpose of design. The research model is a function of cohesion ( $C_u$ ) and angle of internal friction ( $\phi$ ) which are dependent on depth ( $d$ ), unit weight of soil ( $\gamma$ ), liquid limit (LL), plastic limit (PL). The use of Python computer aided software and Microsoft excel was of huge significance in this research.

Mathematical models were developed utilizing the least squares approach, implemented through Python scripting, to predict both the cohesion and the angle of internal friction of soil at any arbitrary depth. The parameters of cohesion and the angle of internal friction are expressed as functions of soil depth( $D$ ), along with liquid limit (LL), plastic limit (PL), and the effective unit weight of the soil ( $\gamma'$ ).  $a, b, c, d$  and  $e$  are constants.

Equation (3.1) presents the model for the prediction of Cohesion.

$$1 + C_u = a(1 + D)^b(1 + W)^c(1 + P)^d(\gamma')^e \tag{1}$$

Linearizing Equation (1) yields Equation (2)

$$\ln(1 + C_u) = \ln a + b \ln(1 + D) + c \ln(1 + W) + d \ln(1 + P) + e \ln(\gamma') \tag{2}$$

The solution matrix for Cohesion is given in Equation (3)

$$\left\{ \begin{array}{l} \sum_{i=1}^n \ln(1 + C_u) \\ \sum_{i=1}^n \ln(1 + C_u) \ln(1 + D) \\ \sum_{i=1}^n \ln(1 + C_u) \ln(1 + W) \\ \sum_{i=1}^n \ln(1 + C_u) \ln(1 + P) \\ \sum_{i=1}^n \ln(1 + C_u) \ln(\gamma') \end{array} \right\} =$$

$$\left[ \begin{array}{ccccc} n & \sum_{i=1}^n \ln(1 + D) & \sum_{i=1}^n \ln(1 + W) & \sum_{i=1}^n \ln(1 + P) & \sum_{i=1}^n \ln(\gamma') \\ \sum_{i=1}^n \ln(1 + D) & \sum_{i=1}^n [\ln(1 + D)]^2 & \sum_{i=1}^n \ln(1 + D) \ln(1 + W) & \sum_{i=1}^n \ln(1 + D) \ln(1 + P) & \sum_{i=1}^n \ln(1 + D) \ln(\gamma') \\ \sum_{i=1}^n \ln(1 + W) & \sum_{i=1}^n \ln(1 + W) \ln(1 + D) & \sum_{i=1}^n [\ln(1 + W)]^2 & \sum_{i=1}^n \ln(1 + W) \ln(1 + P) & \sum_{i=1}^n \ln(1 + W) \ln(\gamma') \\ \sum_{i=1}^n \ln(1 + P) & \sum_{i=1}^n \ln(1 + P) \ln(1 + D) & \sum_{i=1}^n \ln(1 + P) \ln(1 + W) & \sum_{i=1}^n [\ln(1 + P)]^2 & \sum_{i=1}^n \ln(1 + P) \ln(\gamma') \\ \sum_{i=1}^n \ln(\gamma') & \sum_{i=1}^n \ln(\gamma') \ln(1 + D) & \sum_{i=1}^n \ln(\gamma') \ln(1 + W) & \sum_{i=1}^n \ln(\gamma') \ln(1 + P) & \sum_{i=1}^n [\ln(\gamma')]^2 \end{array} \right] \begin{Bmatrix} lna \\ lb \\ lc \\ ld \\ le \end{Bmatrix} \quad (3)$$

Equation (3.4) presents the model for the prediction of Angle of internal friction.

$$\tan(1 + \phi) = a(1 + D)^b (1 + W)^c (1 + P)^d (\gamma')^e \quad (4)$$

Linearizing Equation (3.4) yields Equation (3.5)

$$\ln[\tan(1 + \phi)] = lna + bln(1 + D) + cln(1 + W) + dln(1 + P) + eln(\gamma') \quad (5)$$

The solution matrix for Cohesion is given in Equation (3.6)

$$\left\{ \begin{array}{l} \sum_{i=1}^n \ln[\tan(1 + \phi)] \\ \sum_{i=1}^n \ln[\tan(1 + \phi)] \ln(1 + D) \\ \sum_{i=1}^n \ln[\tan(1 + \phi)] \ln(1 + W) \\ \sum_{i=1}^n \ln[\tan(1 + \phi)] \ln(1 + P) \\ \sum_{i=1}^n \ln[\tan(1 + \phi)] \ln(\gamma') \end{array} \right\} =$$

$$\left[ \begin{array}{ccccc}
 n & \sum_{i=1}^n \ln(1+D) & \sum_{i=1}^n \ln(1+W) & \sum_{i=1}^n \ln(1+P) & \sum_{i=1}^n \ln(\gamma') \\
 \sum_{i=1}^n \ln(1+D) & \sum_{i=1}^n [\ln(1+D)]^2 & \sum_{i=1}^n \ln(1+D)\ln(1+W) & \sum_{i=1}^n \ln(1+D)\ln(1+P) & \sum_{i=1}^n \ln(1+D)\ln(\gamma') \\
 \sum_{i=1}^n \ln(1+W) & \sum_{i=1}^n \ln(1+W)\ln(1+D) & \sum_{i=1}^n [\ln(1+W)]^2 & \sum_{i=1}^n \ln(1+W)\ln(1+P) & \sum_{i=1}^n \ln(1+W)\ln(\gamma') \\
 \sum_{i=1}^n \ln(1+P) & \sum_{i=1}^n \ln(1+P)\ln(1+D) & \sum_{i=1}^n \ln(1+P)\ln(1+W) & \sum_{i=1}^n [\ln(1+P)]^2 & \sum_{i=1}^n \ln(1+P)\ln(\gamma') \\
 \sum_{i=1}^n \ln(\gamma') & \sum_{i=1}^n \ln(\gamma')\ln(1+D) & \sum_{i=1}^n \ln(\gamma')\ln(1+W) & \sum_{i=1}^n \ln(\gamma')\ln(1+P) & \sum_{i=1}^n [\ln(\gamma')]^2
 \end{array} \right] \left. \begin{array}{l} \{ \\ \ln a \\ b \\ c \\ d \\ e \} \end{array} \right\} (6)$$

III. RESULTS AND DISCUSSION

The experimental data obtained from laboratory site investigations in the study areas were compiled and referred to as "Experimental Results." These results were subsequently employed in the model to generate simulated outcomes at varying depths, termed "Predicted Results." Both sets of data are presented in Tables 1 and 2. The predicted values of cohesion (Cu) and angle of internal friction (φ) detailed in Tables 1 to 2 are accompanied by the corresponding independent soil parameters derived from the modeling program developed using python scripting.

Table 1 Experimental Results from Assa Gas Plant Geotechnical Field Investigation

BH No.	Depth (m)	Moisture content (%)	Bulk/Effective Unit Weight(KN/m <sup>3</sup> )	Dry Unit Weight (KN/m <sup>3</sup> )	Undrained strength Cu (KN/m <sup>3</sup> )	Angle of Int. friction Ø (Deg.)	Liquid limit (%)	Plastic limit (%)	Plasticity Index (%)
1	1.5	18.5	17.1	14.4	63	14	25	15	10
	3	18.6	19.2	17	57	14	23	16	7
	4.5	18.6	18.3	15.4	52	22	36	22	14
	7.5	17.1	18.1	16	50	16	37	23	14
2	4.5	18.8	18.9	15.9	73	10	28	16	12
	6	18.4	18.2	15.2	50	13	26	14	12
	7.5	19.4	20.4	17.1	74	9	29	14	15
3	10.5	21.7	19.6	16.1	91	9	31	15	16
	1.5	18.7	17.2	14.6	58	12	24	14	10
	3	18.5	20.1	17	57	14	35	16	19
	4.5	18.6	18.8	15.9	63	7	27	19	8
4	6	20.7	19.3	16	67	9	32	18	14
	1.5	26.5	19.4	15.3	56	10	15	5	10
	3	23.8	19.6	15.8	86	13	21	12	9
	4.5	22.4	19.6	16	101	6	33	16	17
5	6	20.3	19.7	16.2	67	10	34	16	18
	1.5	24.5	19.3	15.7	56	8	28	18	10
	3	21.9	18.8	15.4	84	14	29	20	9
	6	13.7	19.9	17.5	79	20	38	26	12
6	9	20.6	20	16.6	106	8	37	29	8
	1.5	16.8	19.8	16.9	101	16	27	19	8
	3	18.6	19.2	17.1	58	12	30	19	11
	4.5	17.3	20	17.1	110	10	42	27	15
	7.5	12.2	20.8	18.5	96	17	44	27	17
	1.5	19.1	19.3	17.5	61	9	34	22	12

7	3	18.5	19.8	16.7	69	18	34	25	9
	6	21.5	18.2	15	89	6	24	18	6
	9	19.5	19.1	16	103	7	36	24	12
	1.5	17.4	18.2	15.5	64	14	32	15	17
8	4.5	18.3	20.1	16.9	58	21	31	16	15
	7.5	18.8	18.9	15.9	53	19	35	22	13
	10.5	16.8	19.5	16.7	63	18	30	21	9
	1.5	19.2	18.6	16.3	60	10	38	25	13
9	6	21.9	19.8	16.2	103	11	34	26	8
	9	11.8	17	15.2	89	17	31	21	10
	10.5	17.7	19.4	16.5	104	4	34	17	17
	1.5	21.5	18.7	16.2	54	6	38	19	19
10	3	21.4	19.2	15.8	100	6	35	21	14
	4.5	20.1	19.3	15.9	68	11	37	19	18
	6	22.9	18.7	15.2	100	6	34	23	11
	1.5	19.8	19.3	16.1	80	8	26	16	10
11	3	20.2	19.8	16.5	67	11	29	20	9
	4.5	11.6	18.9	16.9	56	10	35	25	10
	6	20.4	19.7	16.4	61	12	41	29	12
	1.5	21	19.5	16.1	62	8	39	20	19
12	4.5	11.3	19	17.1	105	11	38	23	15
	7.5	19.4	19.4	16.2	61	15	39	22	17
	10.5	20.1	20.4	16.9	69	19	40	24	16
	1.5	18.8	19.9	16.8	74	12	25	12	13
13	3	20.4	19.8	16.4	55	12	23	12	11
	4.5	20.1	19.5	16.2	77	12	40	31	9
	7.5	19.9	19.7	16.4	67	16	42	31	11
	1.5	20.1	19.1	15.9	58	11	31	17	14
14	6	19.7	19.2	16	102	8	34	20	14
	9	19.7	19.5	16.3	97	9	35	27	8
	12	18.8	19.9	16.8	80	15	33	25	8
	1.5	21.1	19.2	15.9	58	7	36	21	15
15	6	19.4	18.9	15.8	67	12	37	21	16
	7.5	18.4	20.4	17.2	79	14	35	27	8
	9	19.4	20.8	17.4	78	11	31	18	13
	1.5	19.7	19.8	16.5	63	6	29	15	14
16	3	24.4	19.3	15.5	75	14	32	20	12
	6	17	18.1	15.5	81	11	31	19	12
	9	17.5	18.8	16	73	9	34	21	13

**Table 2 Predicted results of Increase in Liquid Limit, Plastic Limit, Effective Unit Weight and Depth**

Depth d(m)	Liquid limit(%)	Plastic limit(%)	Unit Weight, $\gamma$ (kN/m <sup>3</sup> )	Predicted (kN/m <sup>2</sup> )	Cu	Predicted ( $\phi^{\circ}$ )
0	0	0	10	1.324711871	42.201415	
0.1	1	0.5	10.15	2.899622493	24.616747	

0.2	2	1	10.3	4.235098689	17.912738
	3	1.5	10.45	5.457206596	14.426187
0.3					
0.4	4	2	10.6	6.618569571	12.273678
0.5	5	2.5	10.75	7.746331215	10.80154
0.6	6	3	10.9	8.856387742	9.7250866
0.7	7	3.5	11.05	9.958885225	8.9003098
0.8	8	4	11.2	11.06071892	8.2462969
0.9	9	4.5	11.35	12.16680562	7.7139247
1	10	5	11.5	13.28078796	7.2715452
1.1	11	5.5	11.65	14.40545029	6.8977907
1.2	12	6	11.8	15.54297743	6.5776765
1.3	13	6.5	11.95	16.69512241	6.3003603
1.4	14	7	12.1	17.86331928	6.0577891
1.5	15	7.5	12.25	19.04876123	5.8438462
1.6	16	8	12.4	20.25245609	5.6537962
1.7	17	8.5	12.55	21.4752666	5.4839114
1.8	18	9	12.7	22.71794036	5.331214
1.9	19	9.5	12.85	23.98113226	
2	20	10	13	25.26542177	5.1932947
2.1	21	10.5	13.15	26.57132629	5.0681814
2.2	22	11	13.3	27.89931167	4.9542433
2.3	23	11.5	13.45	29.24980056	4.850119
2.4	24	12	13.6	30.62317913	4.754663
2.5	25	12.5	13.75	32.01980247	4.6669035
2.6	26	13	13.9	33.43999906	4.5860105
2.7	27	13.5	14.05	34.88407444	4.5112708
2.8	28	14	14.2	36.3523142	4.4420675
2.9	29	14.5	14.35	37.84498658	4.3778645
3	30	15	14.5	39.36234457	4.3181933
3.1	31	15.5	14.65	40.90462773	4.2626427
3.2	32	16	14.8	42.47206371	4.2108501
3.3	33	16.5	14.95	44.06486959	4.1624947
3.4	34	17	15.1	45.683253	4.1172912
3.5	35	17.5	15.25	47.32741307	4.0749852
3.6	36	18	15.4	48.99754134	4.0353494
3.7	37	18.5	15.55	50.69382242	3.9981793
3.8	38	19	15.7	52.41643468	3.963291
3.9	39	19.5	15.85	54.16555081	3.9305187
4	40	20	16	55.94133832	3.899712
4.1	41	20.5	16.15	57.74395995	3.8707344
4.2	42	21	16.3	59.57357409	3.843462
4.3	43	21.5	16.45	61.43033514	3.8177817
4.4	44	22	16.6	63.31439375	3.79359
4.5	45	22.5	16.75	65.2258972	3.7707924
					3.7493019

4.6	46	23	16.9	67.16498954	3.729039
4.7	47	23.5	17.05	69.13181189	3.7099299
4.8	48	24	17.2	71.1265026	3.691907
4.9	49	24.5	17.35	73.14919746	3.6749077
5	50	25	17.5	75.20002984	3.658874
5.1	51	25.5	17.65	77.27913084	3.6437523
5.2	52	26	17.8	79.38662945	3.6294926
5.3	53	26.5	17.95	81.52265264	3.6160487
5.4	54	27	18.1	83.6873255	3.6033774
5.5	55	27.5	18.25	85.88077133	3.5914387
5.6	56	28	18.4	88.10311174	3.580195
5.7	57	28.5	18.55	90.35446672	3.5696113
5.8	58	29	18.7	92.63495475	3.5596549
5.9	59	29.5	18.85	94.94469287	3.5502951
6	60	30	19	97.28379669	4.6141503
6.1	61	30.5	19.15	99.65238055	3.5332524
6.2	62	31	19.3	102.0505575	3.5255171
6.3	63	31.5	19.45	104.4784394	3.5182737
6.4	64	32	19.6	106.9361369	3.5114998
6.5	65	32.5	19.75	109.4237596	3.5051742
6.6	66	33	19.9	111.941416	3.4992771
6.7	67	33.5	20.05	114.4892137	3.4937897
6.8	68	34	20.2	117.067259	3.4886944
6.9	69	34.5	20.35	119.6756576	3.4839743
7	70	35	20.5	122.314514	3.4796137
7.1	71	35.5	20.65	124.983932	3.4755976
7.2	72	36	20.8	127.6840145	3.4719117
7.3	73	36.5	20.95	130.4148636	3.4685427
7.4	74	37	21.1	133.1765804	3.4654778
7.5	75	37.5	21.25	135.9692654	3.4627048
7.6	76	38	21.4	138.7930184	3.4602122
7.7	77	38.5	21.55	141.6479383	3.4579892
7.8	78	39	21.7	144.5341233	3.4560254
7.9	79	39.5	21.85	147.4516711	3.4543108
8	80	40	22	150.4006784	3.452836
8.1	81	40.5	22.15	153.3812417	3.4515921
8.2	82	41	22.3	156.3934563	3.4505704
8.3	83	41.5	22.45	159.4374174	3.4497629
8.4	84	42	22.6	162.5132193	3.4491618
8.5	85	42.5	22.75	165.6209556	3.4487596
8.6	86	43	22.9	168.7607197	3.4485493
8.7	87	43.5	23.05	171.9326041	3.4485239
8.8	88	44	23.2	175.1367009	3.4486772
8.9	89	44.5	23.35	178.3731016	3.4490028

9	90	45	23.5	181.6418971	3.4494948
9.1	91	45.5	23.65	184.9431781	3.4501475
9.2	92	46	23.8	188.2770343	3.4509555
9.3	93	46.5	23.95	191.6435553	3.4519136
9.4	94	47	24.1	195.04283	3.4530167
9.5	95	47.5	24.25	198.474947	3.45426
9.6	96	48	24.4	201.9399942	3.455639
9.7	97	48.5	24.55	205.4380593	3.4571492
9.8	98	49	24.7	208.9692292	3.4587864
9.9	99	49.5	24.85	212.5335907	3.4605465
10	100	50	25	216.13123	3.4624256

**Experimental Test Results for Cohesion (Cu)**

The result for the cohesion is a representation of Cu values obtained from laboratory investigation at different points and with varying depths, liquid limit, plastic limits and unit weight, the plot showing the Cu values changing with respect to spatial depths and the varying soil parameters at 16 boreholes points in the study areas, as shown in Fig. 2.

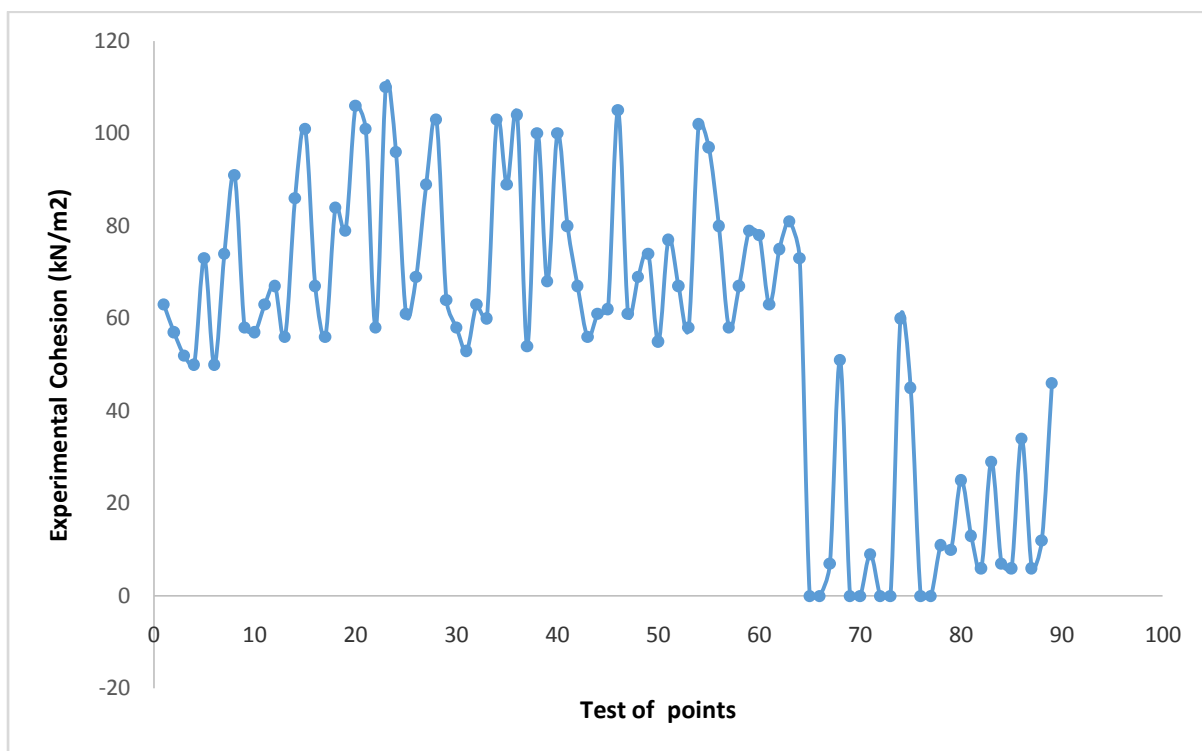


Fig. 2. Experimental Test Results for Cohesion (Cu)

**Experimental Test Results for Angle of Internal Friction**

The angle of internal friction ( $\phi$ ) represents values derived from laboratory investigations conducted at various depths and locations. These values were influenced by changes in liquid limit, plastic limit, and unit weight across the study area. A plot illustrates the variability of  $\phi$  with respect to spatial depth, reflecting the different soil parameters measured at 16 borehole locations within the region as shown in Fig. 3.

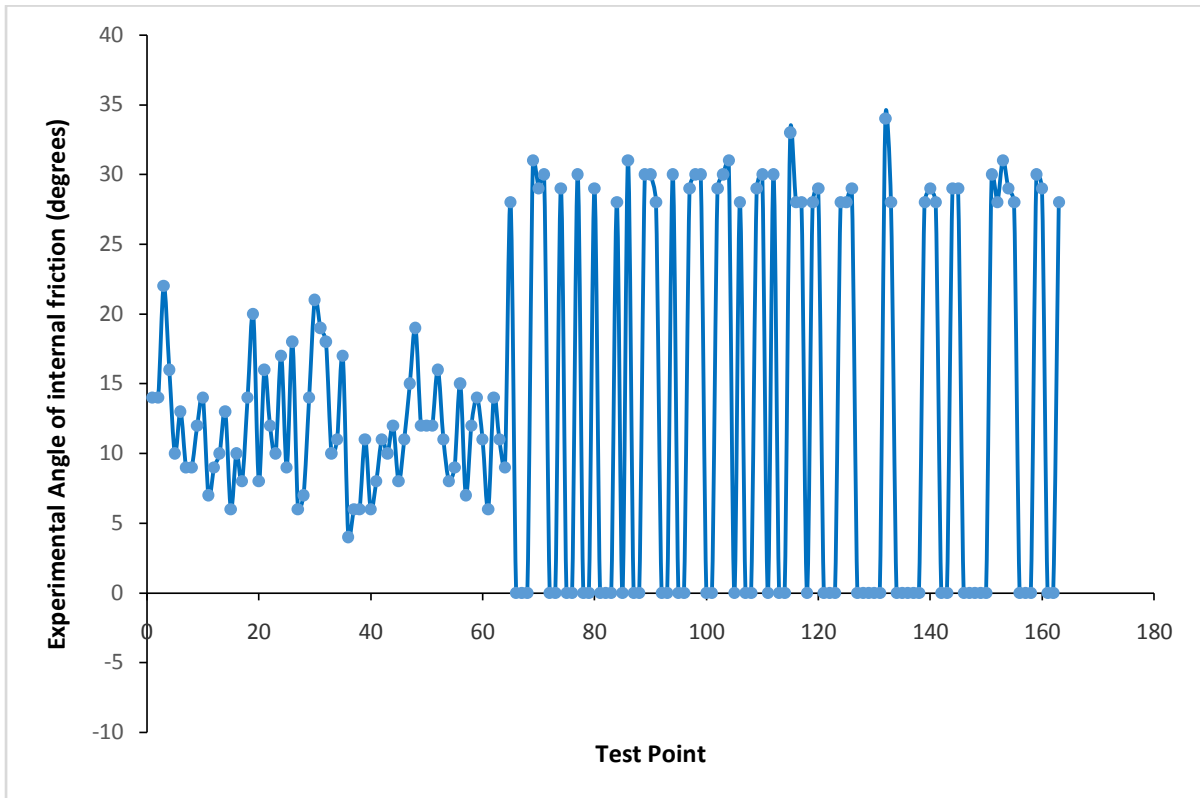


Fig. 3. Experimental Test Results for Angle of Internal friction ( $\phi$ )

**Modelled Results of Cohesion And Angle of Internal Friction**

The computed values for cohesion ( $C_u$ ) and the angle of internal friction ( $\gamma$ ) were derived using empirical models as outlined in equations (1) and (2). These models were specifically developed to estimate the cohesion and angle of internal friction at any specified location, utilising experimental soil property data. The analysis was performed employing the Least Squares method, alongside Python and Microsoft Excel, facilitating both analysis and simulation processes.

$$C_u = 0.041346(1 + D)^{0.1145} (1 + W)^{0.9489} (1 + P)^{-0.4375} (\gamma')^{1.7499} - 1 \tag{1}$$

$$\tan(1 + \phi) = 0.04382(1 + D)^{-0.3005} (1 + W)^{-1.6362} (1 + P)^{1.1609} (\gamma')^{1.3311} \tag{2}$$

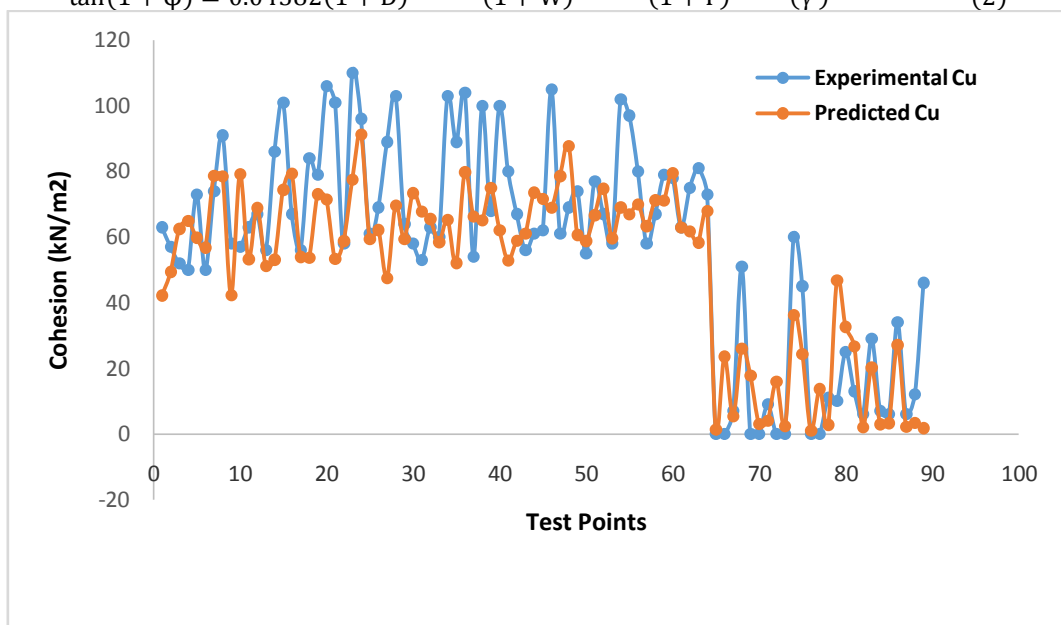


Fig. 3. Experimental Test Results for Experimental and Predicted ( $C_u$ )

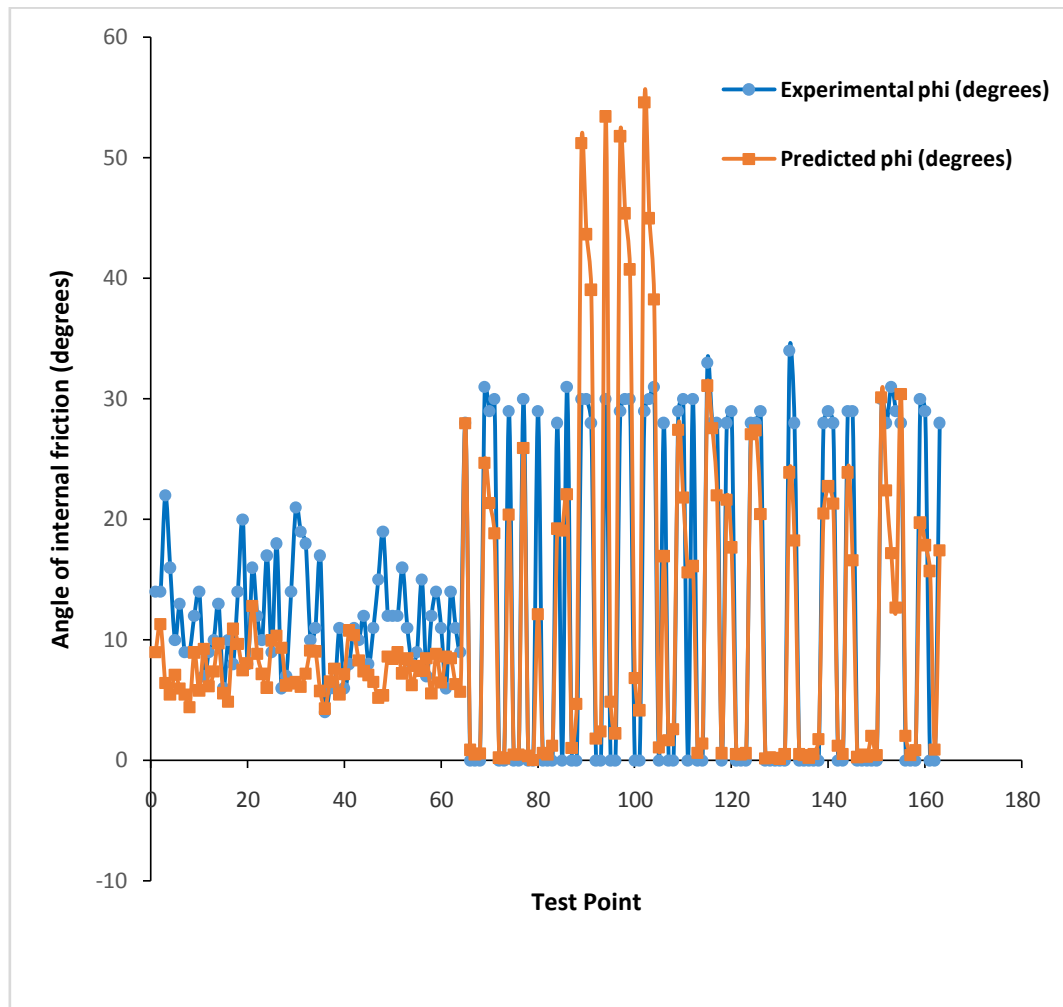


Fig. 4. Experimental Test Results for experimental and predicted ( $\phi$ )

Furthermore the model reveals the experimental and predicted results of  $C_u$  and  $\gamma$  values shows reliability as the graphs of both experimental and predicted values are in close range as shown in Fig. 3 and Fig. 4.

#### **Prediction of Cohesion and Angle of Internal Friction with Decreasing Liquid Limit, Plastic Limit, and Increasing Effective Unit Weight and Depth.**

The analysis of the relationship between the decrease in liquid and plastic limits and the increase in effective unit weight and depth indicates a trend of increasing values of cohesion ( $C_u$ ) and the friction angle ( $\phi$ ) that eventually begins to diminish at greater depths. This pattern suggests that the observed changes in  $C_u$  and  $\phi$  are not solely a function of depth, but also influenced by the specific soil properties at those depths.

For instance, at a depth of 5.4 metres, the liquid limit (LL) is measured at 46, the plastic limit (PL) at 23, and the unit weight ( $\gamma$ ) at  $18.1 \text{ kN/m}^3$ , resulting in  $C_u$  and  $\phi$  values of 77.0 and 3.97, respectively. When the depth increases to 5.8 metres, the LL decreases to 42, the PL to 21.0, while the  $\gamma$  increases to  $18.7 \text{ kN/m}^3$ , yielding  $C_u$  and  $\phi$  values of 78.4 and 4.33, correspondingly. At a further depth of 6.4 metres, the LL is 36, the PL is 18, and the  $\gamma$  reaches  $19.6 \text{ kN/m}^3$ , resulting in  $C_u$  and  $\phi$  values of 79.51 and 4.96, respectively, as detailed in fig. 5-12.

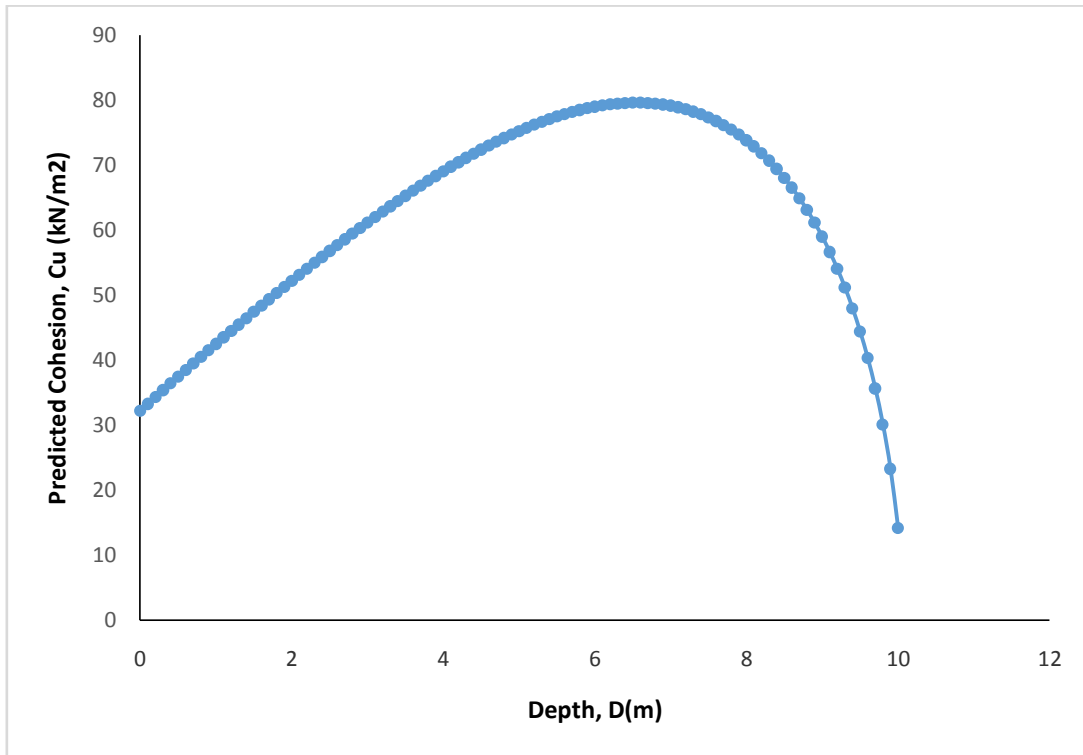


Fig. 5. Prediction of cohesion with increase in depth (d)

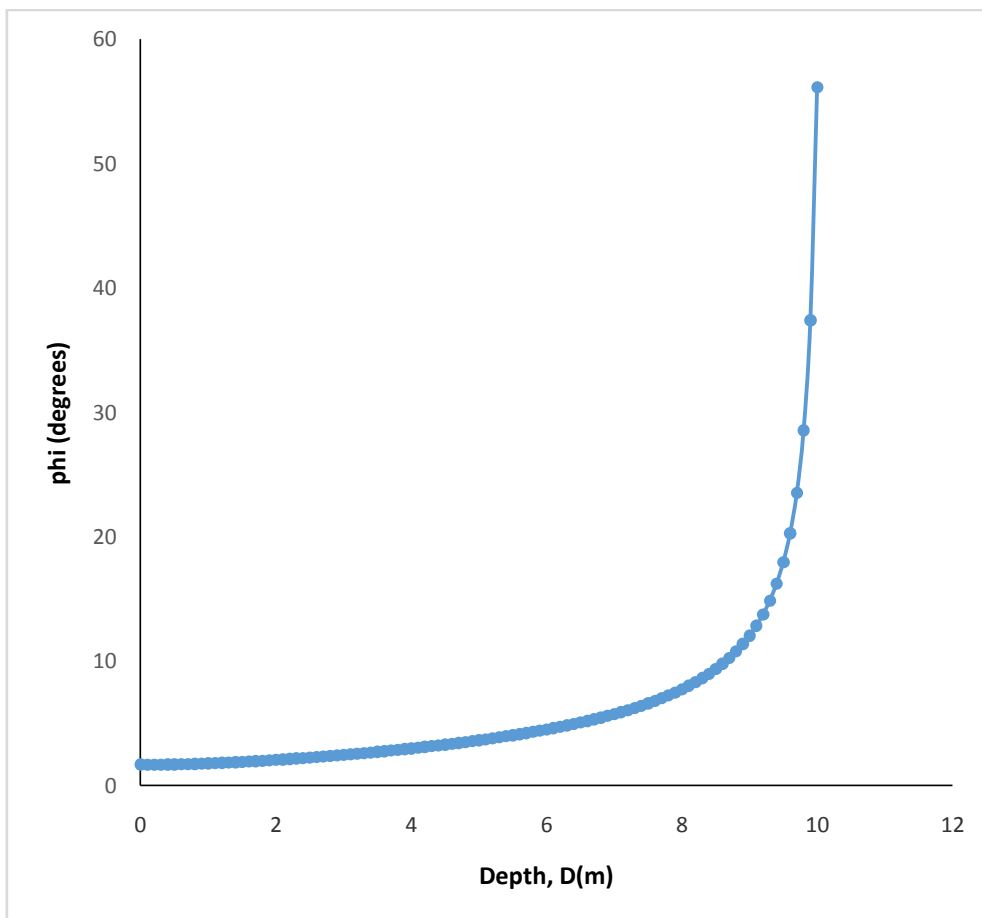


Fig.6. Prediction of angle of internal friction with increase in depth (d)

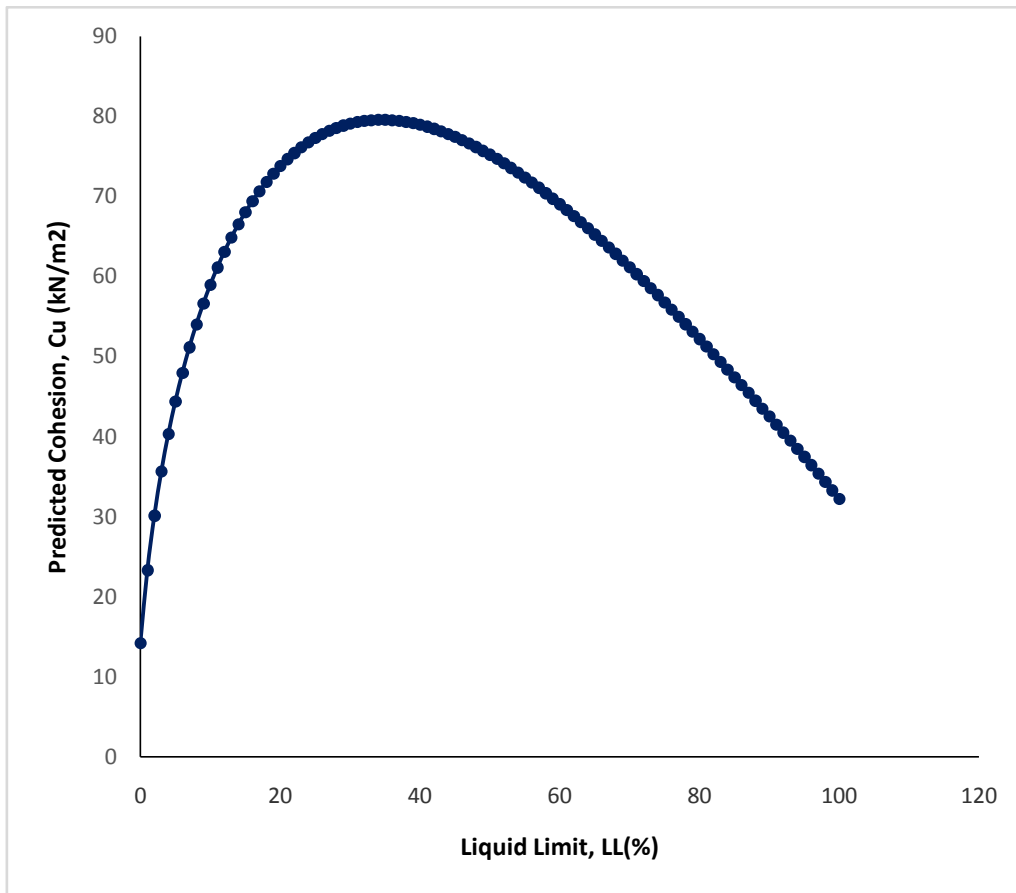


Fig.7. Prediction of cohesion with decrease in liquid limit (LL)

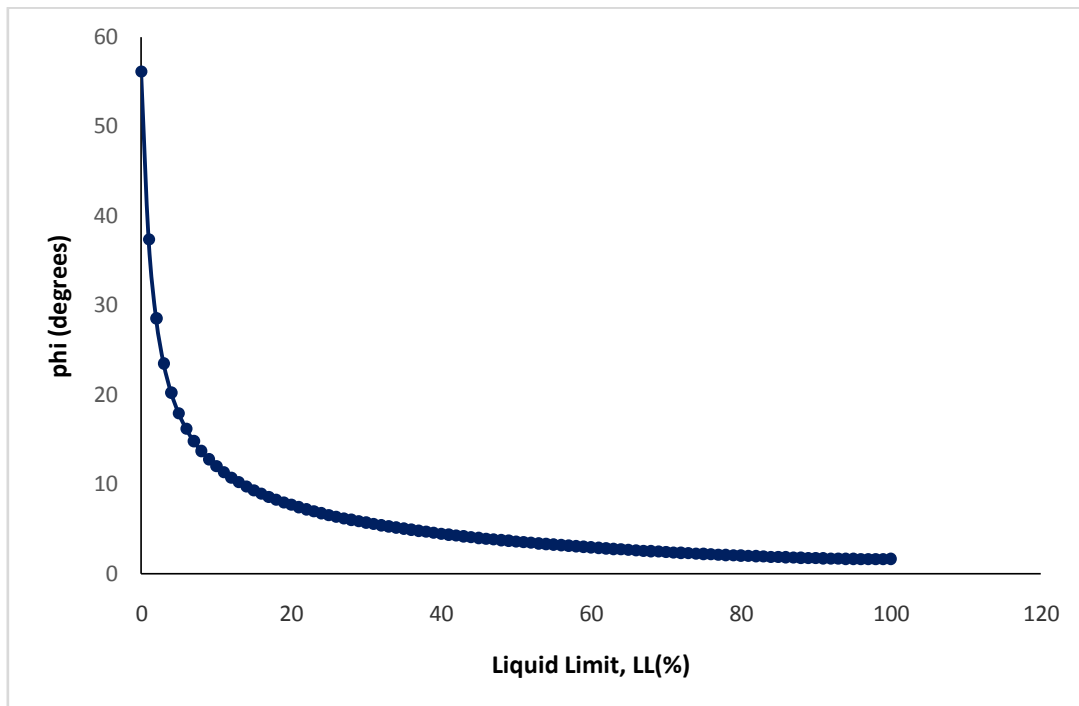


Fig. 8. Prediction of angle of internal friction with decrease in liquid limit (LL)

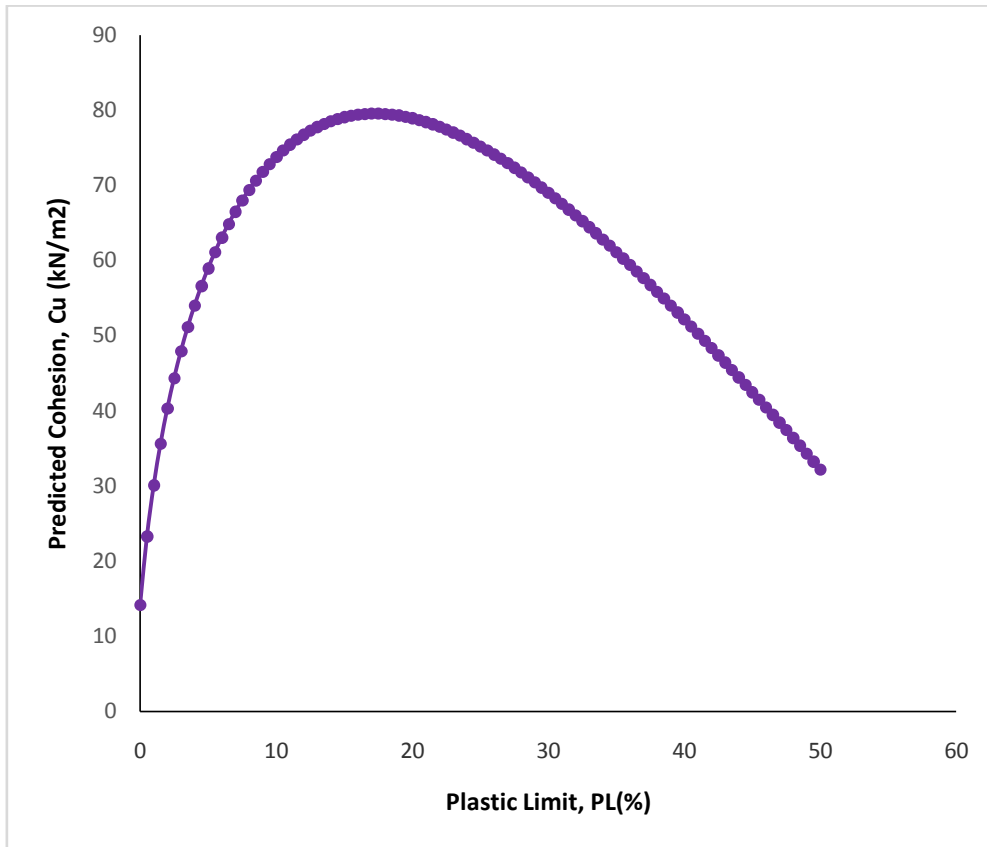


Fig. 9. Prediction of cohesion with decrease in plastic limit (PL)

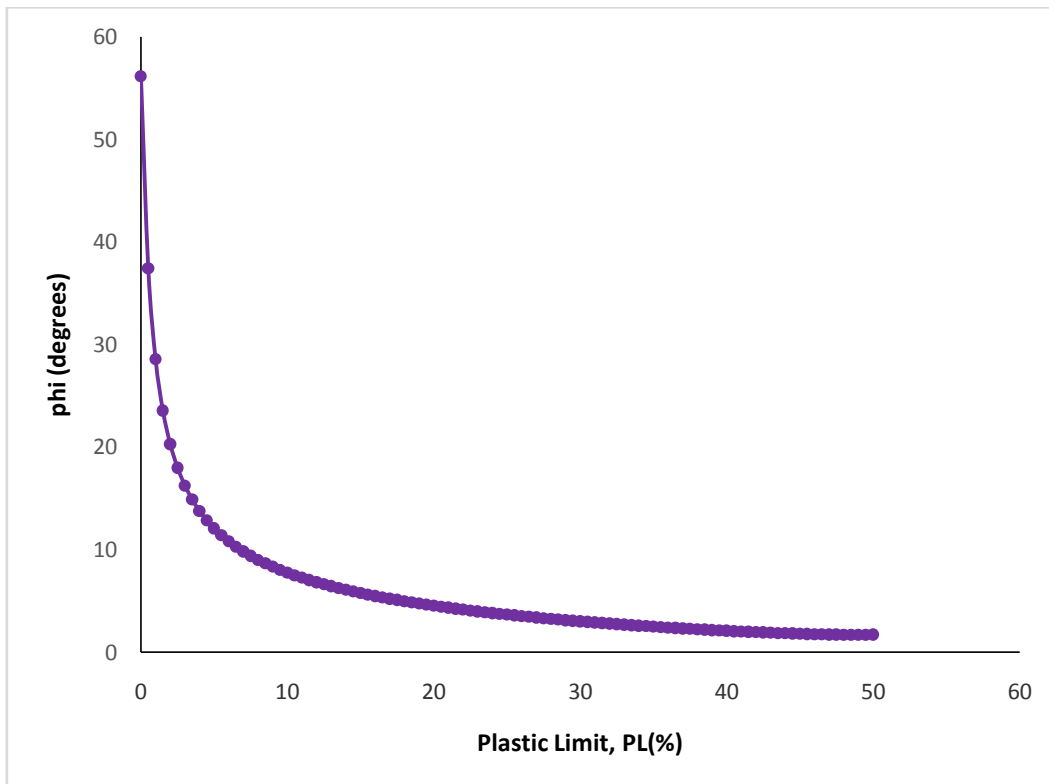


Fig. 10. Prediction of angle of internal friction with decrease in plastic limit (PL)

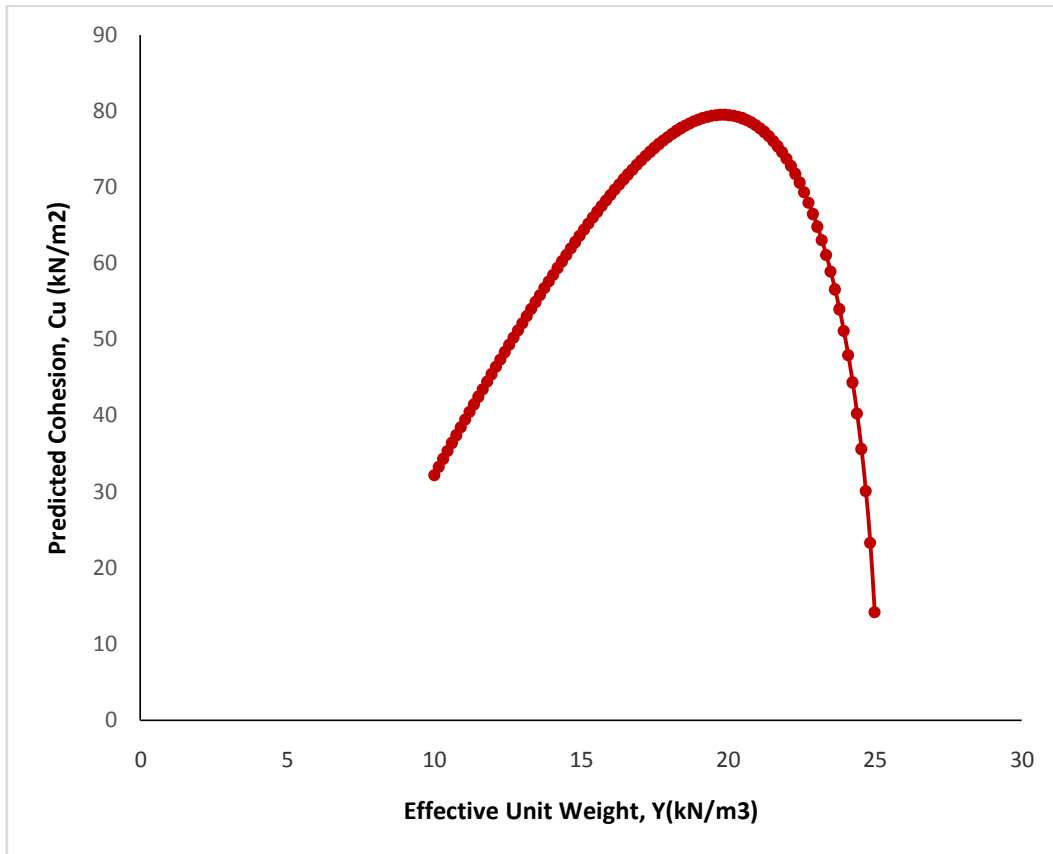


Fig. 11. Prediction of cohesion with increase in effective unit weight ( $\gamma$ )

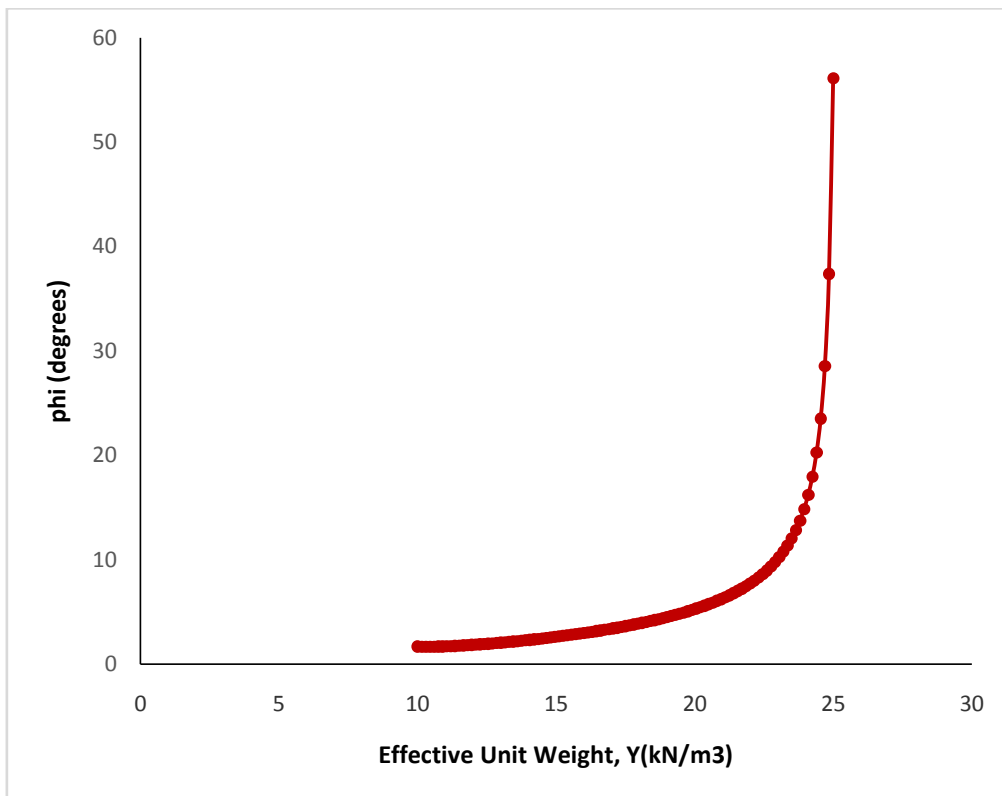


Fig. 12. Prediction of angle of internal friction with increase in effective unit weight ( $\gamma$ )

**Model Validation**

The coefficient of correlation for the experimental and predicted cohesion ( $C_u$ ) across all points and depths,  $r^2 = 0.6846$ , indicating a significance level of 68.4%, compared to coefficient of correlation for the experimental and predicted angle of internal friction ( $\phi$ ),  $r^2 = 0.6526$ , which translates to a significance level of 65.2%. These results reflect a robust correlation, approaching 70% significance threshold and demonstrating a strong degree of reliability in the research.

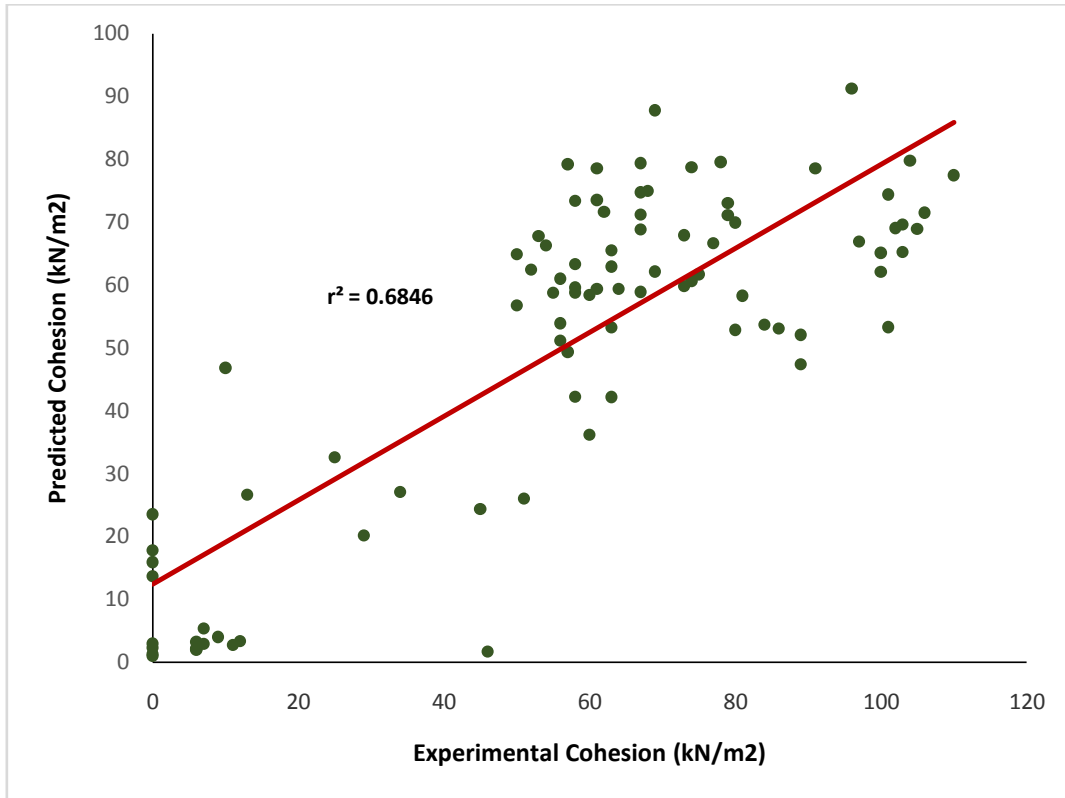


Fig. 13. Correlation coefficient of the experimental and predicted cohesion ( $C_u$ )

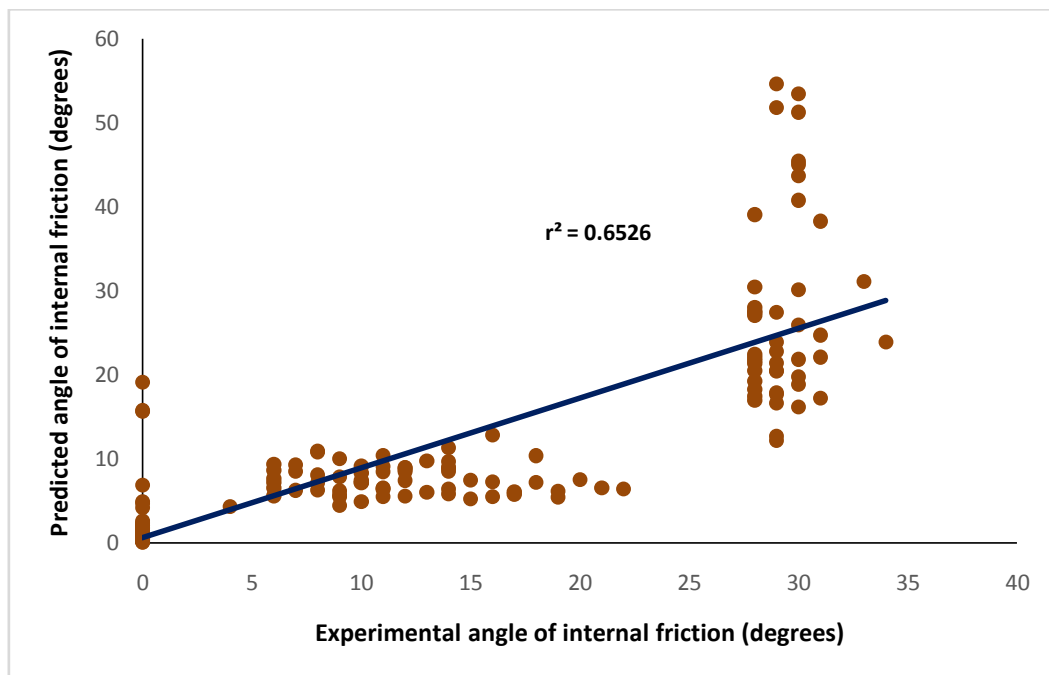


Fig. 14. Correlation coefficient of the experimental and Internal Friction

#### IV. CONCLUSION

The study has demonstrated that modeling in geotechnical engineering can effectively utilise statistical methods, Microsoft Excel, and sophisticated computer modeling tools, such as Python, which was employed in this research. The investigations has established that the model performed reliably, highlighting how experimental soil results can be used to predict reliable geotechnical properties for design purpose. This model establishes a methodology for conducting site-specific investigations through the Least Squares method, implemented in Python software, to determine the undrained cohesion ( $C_u$ ) and angle of internal friction ( $\phi$ ) values of soil at any given site. It also facilitates rapid estimation of the field's undrained cohesion and angle of internal friction at various depths based on the corresponding soil parameters integrated into the model. The study established the direct relationship between index properties, such as liquid limit, plastic limit, alongside the unit weight of soil and depth, as decreasing liquid limit, plastic limit, and increasing effective unit weight, with depth significantly affect the  $C_u$  and  $\phi$  values of the soil. There is an increasing demand for the determination of subsurface geotechnical properties for design purposes. However, the costs associated with field investigations have hindered the practice of exploring greater depths and additional locations on-site. This research tool would provides a cost-effective system for geotechnical field investigations, providing engineers with access to reliable data.

#### References

- [1]. Phoon, K. K., & Kulhawy, F. H. (1999). Characterization of Geotechnical Variability. *Canadian Geotechnical Journal*, 36(4), 612-624.
- [2]. Onyejekwe, S. (2012). "Characterization of soil variability for reliability-based design" Doctoral Dissertations. 2142.
- [3]. Smith, J., & Green, P. (2021). The impact of real-time data on geotechnical modeling. *International Journal of Soil Mechanics*.
- [4]. Jones, A., Smith, T., & Williams, L. (2023). The impact of climate change on groundwater movement: Implications for soil variability. *Journal of Hydrology*, 640, 125437.
- [5]. Li, S., & Kumar, V. (2023). Developing regional standards for geotechnical reliability models. *Journal of Civil Engineering*.
- [6]. Beckie, R. (2021). Enhancing the Predictive Reliability of Soil Models: New Insights and Approaches. *Journal of Geotechnical Engineering*, 54, 120-135
- [7]. Johnson, R. (2021). Remote sensing in geotechnical engineering: A critical review. *International Soil Science Review*.
- [8]. Davis, K., & Liu, X. (2020). Integrating traditional and modern methods for soil variability analysis. *Journal of Geotechnical Advances*.
- [9]. Jiang, L., Tran, H., & Nguyen, T. (2018). Least Squares Method in Parameter Estimation for Geotechnical Engineering. *Engineering Geology Journal*.
- [10]. Smith, R., & Zhang, X. (2020). Expanding the Applications of Least Squares in Geotechnical Engineering. *International Journal of Soil Mechanics*.
- [11]. Doe, J., Smith, A., & Brown, C. (2021). Integrating Machine Learning with Least Squares for Improved Soil Modeling. *Soil Science Advances*.